

Polarization switching in composite-resonator vertical-cavity lasers

D. M. Grasso and K. D. Choquette^{a)}

Department of Electrical and Computer Engineering, University of Illinois at Urbana-Champaign, Urbana, Illinois 61801

(Received 2 June 2003; accepted 30 October 2003)

We report polarization switching in a monolithic dual-resonator vertical-cavity laser. The light output from the top ion-implanted cavity under forward bias above threshold is partitioned into two orthogonal polarizations of the fundamental transverse mode. A reverse bias of sufficient magnitude applied to the bottom oxide-confined cavity causes the abrupt suppression of the dominant polarization and simultaneous emergence of the orthogonal polarization. We find that the electro-optic birefringence of the two polarizations increases with increasing reverse bias. We show that the mechanism of the polarization switch is consistent with wavelength-dependent loss from electroabsorption in the reverse-biased quantum wells of the oxide-confined cavity. © 2003 American Institute of Physics. [DOI: 10.1063/1.1636266]

Vertical-cavity surface-emitting lasers (VCSELs) offer inherent high-speed operation due to their small active volume and low threshold currents.¹ However, because of their typically isotropic transverse cavity geometry, the light output is typically a superposition of two orthogonal polarizations for each transverse mode.^{2,3} The polarization components usually exhibit slightly different frequencies because of several factors, including crystal strain, electro-optic birefringence due to the built-in electric field in the structure, and the spin dynamics of the carriers.^{4,5} In addition, the partitioning of the laser power into the two polarizations is usually unequal, and is influenced by the relative spectral overlap with the material gain.⁶ There has been considerable work in the area of polarization modulation and switching in VCSELs. Polarization modulation has been achieved through a variety of techniques, including anisotropic cavity geometries,⁷ an external cavity with feedback,⁸ and optical injection.⁹ Recently, polarization switching in composite-resonator vertical-cavity lasers (CRVCLs) was reported under pulsed operation.¹⁰

In this letter, we report the polarization properties of a CRVCL under cw operation. A schematic of the device characterized, depicted in the inset of Fig. 1, shows two active, coupled cavities.¹¹ It is grown by metalorganic vapor-phase epitaxy, and is composed of a monolithic bottom distributed Bragg reflector (DBR) with 35 periods, a middle DBR with 14.5 periods, and a top DBR with 21 periods. The mirror layers separate two $1\text{-}\lambda$ -thick optical cavities, each of which contains five GaAs quantum wells (QWs). The top cavity is defined using ion implantation, with an aperture of $6\text{ }\mu\text{m}$. The bottom cavity has an aperture of approximately $10\text{ }\mu\text{m}$, and is defined using selective oxidation. The device is fabricated in a double-mesa structure to allow for independent electrical injection into either cavity.

The additional cavity and middle mirror in the CRVCL have interesting consequences to the spectral output of the device. The middle DBR has a reflectivity of 85%–90%, which implies that an optical field generated in one cavity

will be coupled into the other. This coupling produces two longitudinal resonances, each of which can lase independently with a family of transverse modes.¹² In general, electrical injection into both cavities may be necessary for the laser to reach threshold, since the unpumped QWs in an open circuited cavity will strongly absorb light.¹³ However, for many of the devices characterized in this wafer, the laser will operate with dc injection into only one cavity.

We have obtained cw polarization-resolved light output with a reverse bias applied to one cavity. The top ion-implanted cavity is forward biased above threshold using a precision power supply and the bottom oxide-confined cavity is reverse biased using a semiconductor parameter analyzer. The light output is captured with a Si photodetector and the spectral output is examined using an optical spectrum analyzer with a resolution bandwidth of approximately $0.6\text{ }\text{\AA}$. The output polarizations were distinguished using a linear polarizer. Under these conditions, the output of the device is both single longitudinal and single transverse mode, with $\lambda \approx 900\text{ nm}$. This indicates that the cavity resonances are red-shifted with respect to the peak of the material gain, which is important for the analysis to follow.

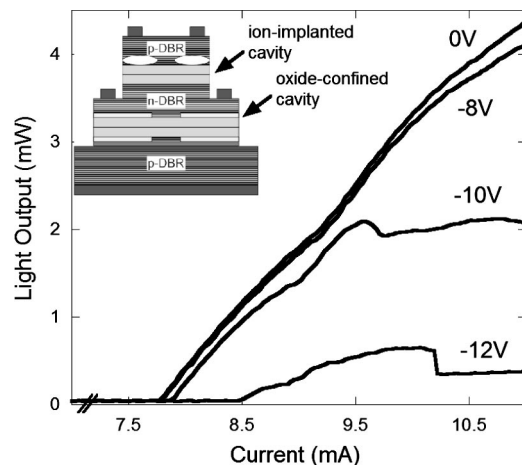


FIG. 1. Light output versus injection current into ion-implanted cavity for various values of reverse bias to oxide-confined cavity. Inset: Device structure for the CRVCL.

^{a)}Electronic mail: choquett@uiuc.edu

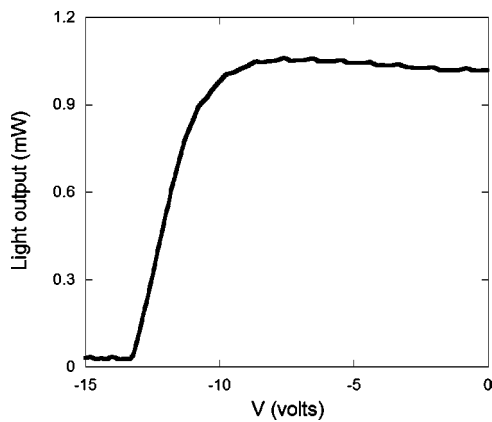


FIG. 2. Light output versus reverse bias in oxide-confined cavity.

Figure 1 shows the cw light output versus injection current only into the ion-implanted cavity with various values of reverse bias in the oxide-confined cavity. An increase in reverse bias in the oxide-confined cavity causes an increase in threshold current and a decrease in differential slope efficiency, consistent with increasing optical loss.

Figure 2 shows the light output of the device for approximately 8 mA of current injected into the top ion-implanted cavity versus reverse bias applied to the oxide-confined cavity. Figure 2 is consistent with previous reports on a CRVCL with a bulk GaAs absorber as a second cavity,¹¹ as well as integrated QW modulators in VCSELs.¹⁴ The reverse breakdown voltage of the oxide-confined cavity is larger than -15 V, so that it is never in the current avalanche breakdown regime during any of our measurements. The general trend of decreasing light output with increasing reverse bias is consistent with the increase in electroabsorption in the reverse-biased QWs.¹⁵

Figure 3 shows an example of the light output versus reverse bias with the two polarizations, p1 and p2, resolved. When the oxide-confined cavity is open circuited, the output of the ion-implanted cavity lases in two orthogonal linear polarization states, with the p1 polarization dominant. As the reverse bias in the oxide-confined cavity is initially increased, the majority of the light is maintained in the dominant p1 polarization, although the partitioning changes slightly. However, at approximately -13 V, there is an abrupt switch, and the p1 state is suppressed in favor of the

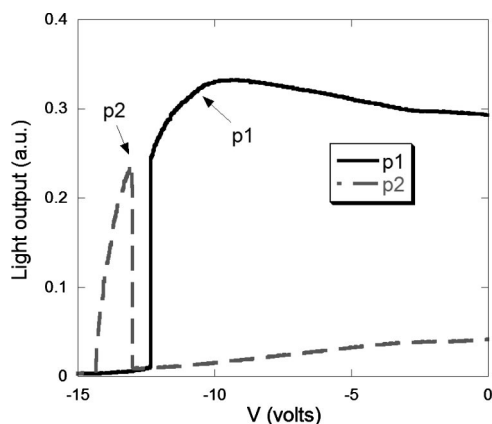


FIG. 3. Polarization resolved light output versus reverse bias in oxide-confined cavity.

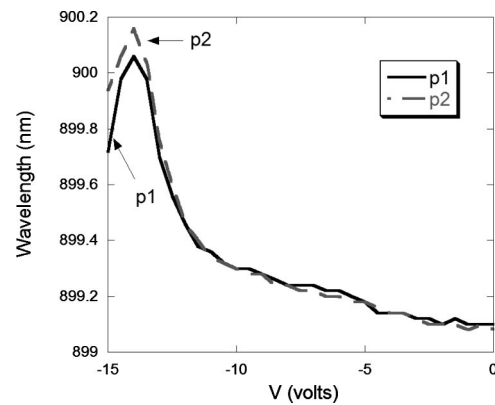


FIG. 4. Spectral evolution versus reverse bias in oxide-confined cavity.

orthogonal polarization p2. For a given device, this switch occurs at slightly different values of reverse bias for repeated sweeps of voltage (which is the cause of the small gap between the turn-off of the p1 state and the turn-on of the p2 state in Fig. 3), and also varies between different devices. Eventually, as the reverse bias is increased beyond -15 V, both p1 and p2 states are extinguished.

Figure 4 shows the wavelengths of the p1 and p2 polarizations versus reverse bias in the oxide-confined cavity. The initial apparent birefringence is smaller than the resolution bandwidth of the optical spectrum analyzer. Near the reverse bias corresponding to the polarization switch, however, there is an increase in the birefringence between p1 and p2 that is larger than the experimental error. It is also notable that near the polarization switch, the orthogonal polarization p2 shifts to a longer wavelength than does p1. Both of these trends have been observed from several CRVCL devices. Since both polarization modes are redshifted with respect to the material gain, the mode with shorter wavelength should have more available gain. Furthermore, upon heating, the peak of the material gain will shift to longer wavelengths.³ Therefore, we do not believe that the polarization switch is caused by the relative spectral overlap of p1 and p2 with the material gain, where the spectral overlap may change with reverse bias in the oxide-confined cavity.

Previous work has analyzed polarization switching in conventional VCSELs by including changes in the gain and loss for the two polarization states.¹⁶ An explanation for the CRVCL polarization switch observed here is wavelength-dependent optical loss from electroabsorption in the reverse-biased QWs. The data in Fig. 4 are consistent with the general trend of decreasing absorption coefficient α for wavelengths longer than the bandgap of bulk GaAs.¹⁵ Herzinger *et al.*¹⁵ calculated the value $\Delta\alpha/\Delta\lambda \sim 1$ to $5 \text{ cm}^{-1}/\text{nm}$, which would produce sufficient excess loss for the shorter wavelength mode to induce a polarization switch (especially given the larger birefringence near -13 V). The increase in wavelength splitting between p1 and p2 observed with increasing reverse bias is presumably due to the electro-optic effect.⁴ This hypothesis implies that the polarization with longer wavelength will encounter less electroabsorption and will therefore become the dominant lasing mode, as observed in Fig. 3.

In summary, we have reported polarization switching under cw operation of a CRVCL with one cavity biased near

threshold and the other reverse biased. Because the two modes are redshifted with respect to the peak material gain, the relative spectral overlap of the two polarizations producing differing modal gain is not the cause of the switch. Our results are consistent with differing optical loss produced by wavelength dependent electroabsorption in the reverse-biased QWs of the oxide-confined cavity. The polarization switching of light in a CRVCL provides an enhanced method for performing optical modulation since the switch can be controlled by an electric field external to the lasing cavity, and thus may not be limited by the relaxation oscillation frequency of the laser. This could offer an alternative to the direct modulation scheme used by laser sources in optical communication systems.

¹K. D. Choquette and K. M. Geib, in *Vertical-Cavity Surface-Emitting Lasers*, edited by C. Wilmsen, H. Temkin, and L. Coldren (Cambridge, New York, 1999), pp. 193–232.

²C. J. Chang-Hasnain, J. P. Harbison, G. Hasnain, A. C. Von Lehmen, L. T. Florez, and N. G. Stoffel, *IEEE J. Quantum Electron.* **27**, 1402 (1991).

³K. D. Choquette, D. A. Ritchie, and R. E. Leibenguth, *Appl. Phys. Lett.* **64**, 2062 (1994).

⁴M. P. van Exter, A. K. Jansen van Doorn, and J. P. Woerdman, *Phys. Rev. A* **56**, 845 (1997).

⁵J. Martin-Regalado, F. Prati, M. San Miguel, and N. B. Abraham, *IEEE J. Quantum Electron.* **33**, 765 (1997).

⁶K. D. Choquette, R. P. Schneider, Jr., K. L. Lear, and R. E. Leibenguth, *IEEE J. Sel. Top. Quantum Electron.* **1**, 661 (1995).

⁷K. D. Choquette, K. L. Lear, R. E. Leibenguth, and M. T. Asom, *Appl. Phys. Lett.* **64**, 2767 (1994).

⁸S. Jiang, Z. Pen, M. Dagenais, R. A. Morgan, and K. Kojima, *Appl. Phys. Lett.* **63**, 3545 (1993).

⁹K. Panajotov, F. Berghmans, M. Peeters, G. Verschaffelt, J. Danckaert, I. Veretennicoff, and H. Thienpont, *IEEE Photonics Technol. Lett.* **11**, 985 (1999).

¹⁰V. Badilita, J. F. Carlin, M. Ilegems, M. Brunner, G. Verschaffelt, and K. P. Panajotov, *Proc. SPIE* **363**, 4942 (2002).

¹¹A. J. Fischer, K. D. Choquette, W. W. Chow, H. Q. Hou, and K. M. Geib, *Appl. Phys. Lett.* **75**, 3020 (1999).

¹²M. Brunner, K. Gulden, R. Hövel, M. Moser, J. F. Carlin, R. P. Stanley, and M. Ilegems, *IEEE Photonics Technol. Lett.* **12**, 1316 (2000).

¹³D. M. Grasso and K. D. Choquette, *IEEE J. Quantum Electron.* **56**, (2003).

¹⁴S. Lim, J. Hudgings, L. Chen, G. Li, W. Yuen, K. Lau, and C. Chang-Hasnain, *IEEE Photonics Technol. Lett.* **10**, 319 (1998).

¹⁵C. M. Herzinger, P. D. Swanson, T. K. Kang, T. M. Cockerill, L. M. Miller, M. E. Givens, T. A. DeTemple, J. J. Coleman, and J. P. Leburton, *Phys. Rev. B* **44**, 13478 (1991).

¹⁶B. Ryvkin, K. Panajotov, A. Georgievski, J. Danckaert, M. Peeters, G. Verschaffelt, H. Thienpont, and I. Veretennicoff, *J. Opt. Soc. Am. B* **16**, 2106 (1999).